Cell, Vol. 97, 621–633, May 28, 1999, Copyright ©1999 by Cell Press

Relocalization of Telomeric Ku and SIR Proteins in Response to DNA Strand Breaks in Yeast

Sophie G. Martin,* Thierry Laroche,*
Noriyuki Suka,† Michael Grunstein,†
and Susan M. Gasser*‡
*Swiss Institute for Experimental Cancer Research
Ch. des Boveresses 155
CH-1066 Epalinges
Switzerland
†Department of Biological Chemistry
UCLA School of Medicine and
Molecular Biology Institute
University of California
Los Angeles, California 90095

Summary

Telomeric TG-rich repeats and their associated proteins protect the termini of eukaryotic chromosomes from end-to-end fusions. Associated with the cap structure at yeast telomeres is a subtelomeric domain of heterochromatin, containing the silent information regulator (SIR) complex. The Ku70/80 heterodimer (yKu) is associated both with the chromosome end and with subtelomeric chromatin. Surprisingly, both yKu and the chromatin-associated Rap1 and SIR proteins are released from telomeres in a *RAD9*-dependent response to DNA damage. yKu is recruited rapidly to double-strand cuts, while low levels of SIR proteins are detected near cleavage sites at later time points. Consistently, yKu- or SIR-deficient strains are hypersensitive to DNA-damaging agents. The release of yKu from telomeric chromatin may allow efficient scanning of the genome for DNA strand breaks.

Introduction

The telomere is a unique structure that serves to protect the termini of linear chromosomes from fusions and degradation. Other ends in DNA, such as breaks caused by ionizing radiation or other DNA-damaging agents, must be repaired to ensure that every chromosomal fragment is linked to a single centromere for equal distribution at mitosis. The induction of a single double-strand break (DSB) will cause cells to arrest in the cell cycle at the DNA damage checkpoint until the break is repaired (Sandell and Zakian, 1993).

One universally conserved mechanism by which cells repair DSB is a process referred to as nonhomologous end joining (NHEJ). This involves three well-characterized protein complexes. One is the Ku heterodimer, which in mammalian cells associates with the ATM-related DNA-stimulated protein kinase (DNA-PK; reviewed in Critchlow and Jackson, 1998). The second is the Mre11/Rad50/Xrs2 complex, which has endo- and exonucleolytic activities thought to process the break for religation (reviewed by Haber, 1998). The third is a complex of Xrcc4 and Ligase IV, both of which are essential for the religation step following DSB repair.

The mammalian Ku70 and Ku86 proteins form a heterodimer that binds the ends of double-stranded DNA with high affinity (reviewed in Dynan and Yoo, 1998). Their role in both DSB repair and V(D)J recombination requires DNA-protein kinase (DNA-PK), which is thought to be targeted to sites of damage by Ku (Lieber et al., 1997). Consistent with this role, mice lacking DNA-PK, or either Ku subunit, are sensitive to ionizing radiation, impaired for growth, and have severe combined immunodeficiency. Intriguingly, primary fibroblasts isolated from Ku-deficient mice also have phenotypes of premature senescence (Nussenzweig et al., 1996; Gu et al., 1997). In yeast, DSBs are most frequently repaired by the *RAD52*-dependent homologous recombination pathway. However, *rad52* strains lacking yKu70p or yKu80p (encoded by *HDF1* and *HDF2*, respectively) are highly sensitive to irradiation (Siede et al., 1996), and strains lacking yKu alone are deficient in end-joining reactions (Mages et al., 1996).

Recently it has been shown that Rad52$^+$ strains lacking either *HDF* gene have defects in telomere maintenance. Notably, the terminal TG1-3 repeat is shorter (Porter et al., 1996; Boulton and Jackson, 1998), stretches of single-strand DNA accumulate at chromosomal ends (Gravel et al., 1998), and yeast telomeres are delocalized from the nuclear periphery (Laroche et al., 1998). Concomitantly, telomere position effect (TPE), which confers transcriptional repression on genes in subtelomeric regions, drops by 10^3-fold. Genetic analyses indicate that *hdf* mutants exacerbate the growth and telomere maintenance defects resulting from mutation of either telomerase (*est2*) or a protein that binds the single-strand telomeric DNA (*cdc13*; Gravel et al., 1998; Nugent et al., 1998; Polotnianka et al., 1998). Moreover, *hdf* mutants aggravate defects provoked by the loss of the Mre11/Rad50/Xrs2 complex, which may process the chromosome end creating the 3′ overhang necessary for telomerase function. These data are consistent with the proposal that yKu helps cap the telomere and/or regulates 3′ end processing enzymes.

The fact that *hdf* mutants are defective in both telomere maintenance and DSB repair suggests the direct involvement of yKu at both sites. However, if true, yKu binding must be able to produce two opposite results: at double-strand breaks, DNA ends are processed and religated, while in the case of telomere maintenance, end-to-end ligation is specifically suppressed. At present, it is unknown whether yKu binds directly at both sites of action, what distinguishes the two complexes, and whether yKu is regulated by the damage response pathway.

Here, we examine the fate of yKu and the nucleosome-binding silent information regulator (SIR) complex (reviewed by Shore, 1998) under conditions of induced DNA damage. Our results support a model in which telomeric heterochromatin serves as a reservoir for

‡To whom correspondence should be addressed (e-mail: sgasser@eliot.unil.ch).

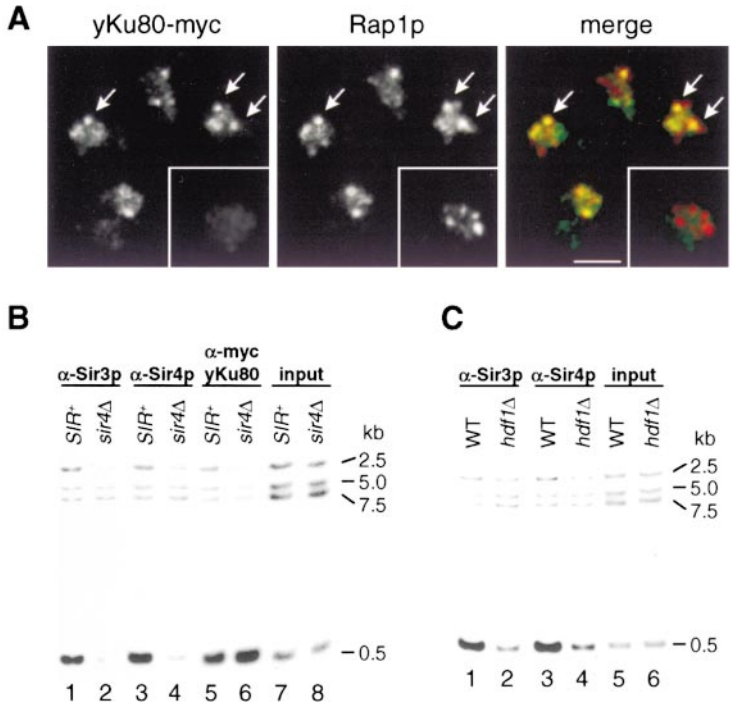

D

kb from TelVI-R end	Sir3p			yKu80-myc		
	wt	*sir4Δ*	ratio	wt	*sir4Δ*	ratio
0.5	3.05	0.65	4.71	4.52	6.98	0.65
2.5	1.65	0.73	2.25	1.52	0.93	1.64
5	1.29	1.19	1.08	1.26	1.31	0.96
7	1	1	1	1	1	1

E

	Sir3p			Sir4p		
	wt	*hdf1Δ*	ratio	wt	*hdf1Δ*	ratio
0.5	6.45	1.41	4.58	5.70	1.68	3.39
2.5	1.89	1.14	1.66	1.52	0.94	1.63
5	1.36	1.28	1.06	1.23	1.13	1.09
7	1	1	1	1	1	1

Figure 1. yKu80p Colocalizes with Rap1p at Telomeric Foci and Binds Telomere Ends in a *SIR4*-Independent Manner

(A) A haploid strain containing a Myc-tagged yKu80p (GA 1009) was stained with anti-Myc (9E10) and anti-Rap1p detected by appropriate fluorescent secondary antibodies. Panels show the anti-Myc signal, the anti-Rap1p signal, and the merge of both signals (yKu80-Myc in green, Rap1p in red, and colocalization in yellow), as indicated. Insets show double labeling of the strain lacking the Myc-tagged *HDF2* gene. Bar, 2 μm.

(B) The chromatin immunoprecipitation (ChrIP) assay was performed as described in Experimental Procedures. Immunoprecipitation was performed with affinity-purified anti-Sir3p (lanes 1 and 2), anti-Sir4p (lanes 3 and 4), and anti-Myc antibodies (9E10, lanes 5 and 6). Radiolabeled PCR using chromosome VI-R primers located at 0.5, 2.5, 5.0, and 7.5 kb from the telomere was performed, and PCR products were resolved on 6% polyacrylamide gels. The strains used were GA1009 (*SIR*$^+$, WT) and GA1061 (*sir4*Δ).

(C) Cross-linking and immunoprecipitation using anti-Sir3p (lanes 1 and 2) and anti-Sir4p polyclonal antibodies (lanes 3 and 4) and radiolabeled PCR were done as described in (B). The strains used were W303A (WT) and YT29 (*hdf1*Δ).

(D) Quantitation of the α-Sir3p and α-yKu80-Myc data shown in (B). Each signal was measured relative to the 7.5 kb signal and normalized to the same ratio in input DNA. Ratio compares *SIR*$^+$ and *sir4*Δ strains.

(E) Quantitation of the data shown in (C). Each signal was measured relative to the 7.5 kb signal and normalized to the same ratio in input DNA. Ratio compares *HDF1*$^+$ and *hdf1*Δ strains.

chromatin factors that respond to physiological signals, such as the *RAD9*-mediated checkpoint.

Results

Ku80p Is Bound to Yeast Telomeres

The yKu heterodimer is implicated in both the proper maintenance of telomere structure and in nonhomologous end-joining reactions that are required to repair DSB in the absence of homologous recombination. Immunoprecipitation data have shown that yeast telomeric DNA repeats can be coimmunoprecipitated with a Myc-tagged yKu80 protein (Gravel et al., 1998), but it was not determined whether this interaction is transient or what happens to yKu when DSB are induced. To study this, we fused a 13-mer Myc epitope to the C terminus of the genomic copy of *HDF2* and performed immunofluorescence studies. Immunostaining with anti-Myc (9E10) antibody reveals that yKu80-Myc is concentrated in a few discrete subnuclear foci per focal plane (Figure 1A).

Double labeling using anti-Myc and affinity-purified anti-Rap1p reveals an extensive colocalization of yKu80p foci with those of the telomere repeat-binding protein Rap1p (signal coincidence is yellow in the merged image, Figure 1A). Since combined immunofluorescence and in situ hybridization have shown that Rap1p foci reflect the clustering of yeast telomeres near the nuclear periphery (Gotta et al., 1996), this colocalization suggests that yKu80p is constitutively enriched at telomeres in wild-type cells.

Both yKu70p and yKu80p are necessary for TPE (Boulton and Jackson, 1998; Laroche et al., 1998). Since yKu70p interacts in a two-hybrid assay with the silent information regulator Sir4p (Tsukamoto et al., 1997), it seemed possible that the telomeric association of yKu might be mediated through its binding to the SIR complex (Sir2p, Sir3p, and Sir4p). To map where yKu binds telomeres, we immunoprecipitated protein–DNA complexes with antibodies recognizing either yKu80-Myc or SIR proteins after cross-linking with formaldehyde in vivo and performed quantitative PCR on the immunoprecipitate with telomere-specific primers (chromatin immunoprecipitation [ChrIP] assay, Strahl-Bolsinger et al., 1997). The terminal 500 bp fragment of Chr. VI-R and a subtelomeric band at 2.5 kb from the telomere end are 4.5- and 1.5-fold enriched in the yKu80-Myc immunoprecipitate as compared to a band produced by primers at 7.5 kb from the telomere end (Figures 1B and 1D). Similarly, in immunoprecipitates of Sir3p or Sir4p, these bands are enriched 3- and 1.5-fold, respectively (Figures 1B and 1D; see also Strahl-Bolsinger et al., 1997). Thus, yKu80p is not only bound to the most distal 500 bp of

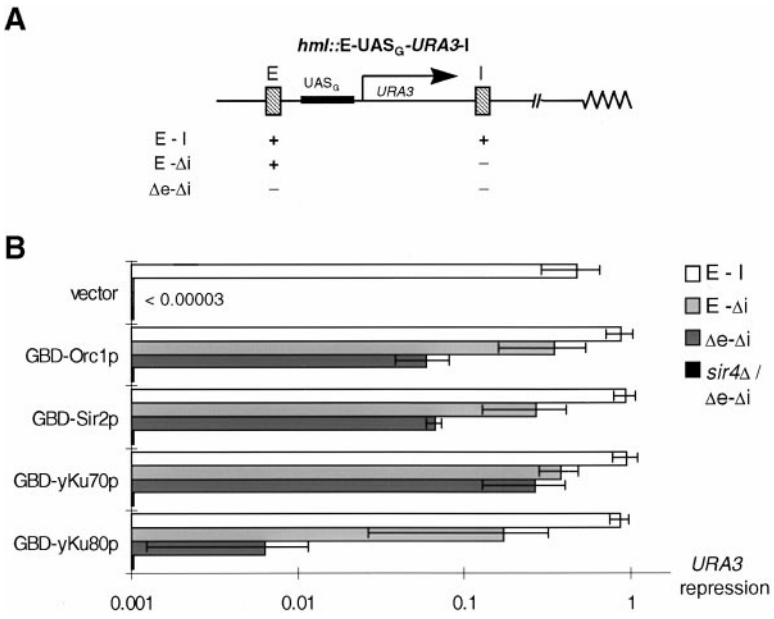

Figure 2. GBD-yKu70p and GBD-yKu80p Nucleate Silencing in the Absence of a Silencer

(A) Targeted repression is monitored in strains that carry *URA3* adjacent to eight Gal4p-binding sites integrated at the *HML* locus, flanked by both the E and I silencers (E-I, white; Ce134), only the E silencer (E-Δi, dashed; Ce76), or neither (Δe-Δi, black; Ce77). These strains were transformed with vectors encoding either yKu80p, yKu70p, Sir2p, or Orc1p fused in-frame to the Gal4 DNA-binding domain (GBD).

(B) The influence of targeted fusion proteins (GBD-yKu70p, GBD-yKu80p, GBD-Sir2p, or GBD-Orc1p) on silencing of the *URA3* gene was monitored as described in Experimental Procedures, as compared to a strain expressing only the GBD (pAS2, vector). The mean and standard deviation were calculated for ratios of cells growing on +FOA and −FOA, for eight independent colonies of each transformant (see bar graph; the x axis represents the efficiency of *URA3* repression in log scale. Less than 3 in 10^5 cells with vector alone grow when one or both silencers are deleted or in a *sir4::HIS3* deletion background (Δe-Δi, *sir4*Δ).

Chr. VI-R, but it appears to spread, like Rap1p and SIR complexes, along the repressed subtelomeric region.

By performing this same assay in a strain deficient for *SIR4* (*sir4*Δ), we find that the association of yKu80-Myc with the more internal sequence is SIR dependent, while its binding to the terminal fragment is not (Figures 1B and 1D). As expected, no association of Sir3p with either telomeric or subtelomeric fragments can be detected in the *sir4*Δ strain. Similarly, Sir3p and Sir4p bind telomeric sequences poorly in an *hdf1*Δ strain (levels are 3- to 5-fold lower than wild-type, Figures 1C and 1E), consistent with the loss of TPE reported for *hdf1* and *hdf2* strains (Laroche et al., 1998). Thus, although yKu has a SIR-independent association with the terminal fragment of the chromosome, it associates with repressed chromatin in a *SIR4*-dependent manner, much like Rap1p (Strahl-Bolsinger et al., 1997).

yKu Can Nucleate Silencing in the Absence of Silencer Elements

The loss of silencing that correlates with *hdf* mutations suggests that yKu might help recruit the SIR complex to subtelomeric chromatin. Moreover, it has been proposed that yKu targets Sir proteins to double-strand breaks, where these latter would perform an as-yet-undefined role in repair (Jackson, 1997; Tsukamoto et al., 1997). To test whether yKu alone can nucleate SIR-mediated repression, we have tethered it by fusion to the Gal4p DNA-binding domain (GBD) to an internal *URA3* reporter placed downstream of a cluster of eight Gal4p recognition sites. The reporter was inserted at *HML*, flanked either by both *HML* E and I silencers, by only the E silencer, or by neither silencer (Figure 2A, E-I, E-Δi, or Δe-Δi). The silencer-flanked *URA3* reporter (E-I) is almost completely repressed in the presence of the GBD alone (vector, Figure 2B), while deletion of one or both silencers results in nearly complete derepression (i.e., lack of growth, as *URA3* expression is toxic on 5-FOA). Constructs with deleted silencers thus allow us to test whether GBD-fusion proteins can establish repression, like the positive controls of Sir2p and Orc1p fused to GBD.

The colony-forming assay on 5-FOA reveals that the GBD-yKu70p is a potent nucleator of repression even in the absence of silencer elements (Figure 2B), silencing *URA3* expression to within 2-fold of the maximal level detected in the two-silencer construct (Figure 2B). Indeed, the GBD-yKu70 fusion nucleates repression more efficiently than GBD-Orc1p or GBD-Sir2p on the construct lacking silencers, while on the construct containing one silencer, all three GBD fusions are equally efficient (Figure 2B). GBD-yKu80p silences as efficiently as GBD-Ku70p on the E-Δi reporter, but it is less efficient on a reporter lacking both silencers, correlating with the fact that GBD-yKu80p only partially complements an *hdf2* deletion, while GBD-yKu70p fully complements an *hdf1* null (data not shown). In all cases yKu-mediated repression is SIR dependent, as no growth is detected on 5-FOA in the absence of Sir4p (see *sir4*Δ, Figure 2B). Furthermore, GBD-yKu70p-mediated silencing requires intact yKu80p (data not shown). It is unlikely that GBD-yKu represses by tethering the reporter to the nuclear envelope (Andrulis et al., 1998), since membrane tethering does not enhance repression in the absence of silencers.

Sir Mutants Are Hypersensitive to DNA-Damaging Agents

Although *hdf* mutants have major telomere phenotypes, the most conserved role of the Ku heterodimer is in nonhomologous end joining during the DSB repair (reviewed in Lieber et al., 1997), just as the primary role of the SIR complex is to confer position-dependent repression on mating type genes. Yet, SIR proteins have also been implicated in the NHEJ reactions monitored by the circularization of linear plasmid DNA (Tsukamoto et al.,

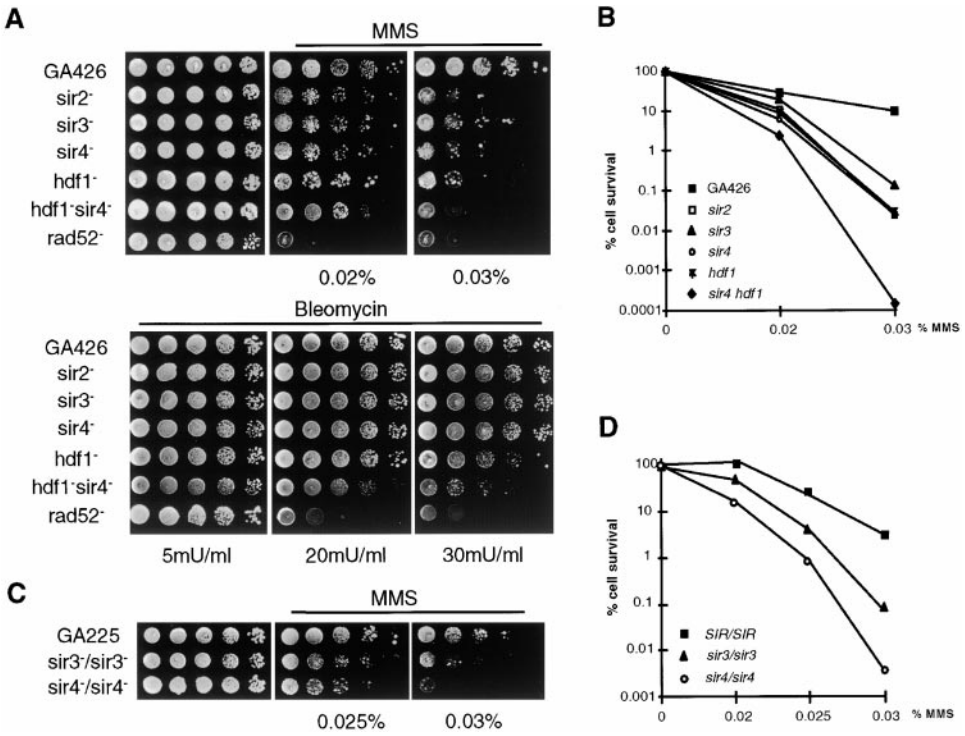

Figure 3. Sensitivity of *hdf* and *sir* Strains to Bleomycin and MMS

(A) Serial 10-fold dilutions of strains derived by gene disruption from the parental strain GA426 were grown on the indicated amounts of bleomycin or MMS (see Experimental Procedures). The following disruptions were performed in GA426: *sir2::HIS3* (sir2$^-$, GA427), *sir3::HIS3* (sir3$^-$, GA428), *sir4::HIS3* (sir4$^-$, GA429), *hdf1::kanMX* (hdf1$^-$, GA911), *hdf1::kanMX sir4::HIS3* (hdf1$^-$ sir4$^-$, GA1065), and *rad52::URA3* (rad52$^-$, GA1050). The *sir* and *rad52* mutants are disruptions and although all *sir* strains have a nonmating phenotype, we cannot exclude that residual expressed domains of the disrupted alleles might be partially functional.

(B) Quantitation of viability on the indicated amounts of MMS are shown for the dilution series shown in (A).

(C) Serial 10-fold dilution series on MMS-containing plates are shown for diploid *sir3* (GA192), *sir4* (GA202), and a congenic *SIR*$^+$ strain (GA225).

(D) Quantitation of viability on the indicated amounts of MMS is shown for the dilution series shown in (C) with additional data from plates containing 0.02% MMS. Hypersensitivity of *sir3* and *sir4* diploids was observed in two other strain backgrounds (data not shown).

1997). In *sir* mutants in a W303 background it has been argued that the drop in NHEJ efficiency reflects the pseudo-diploid state that arises when *HM* silencing is lost (Aström et al., 1999). We therefore examined the viability of both haploid and diploid *sir* mutants in the presence of DNA-damaging agents. A wild-type yeast strain and its isogenic disrupts for *sir2*, *sir3*, *sir4*, *hdf1*, or *rad52* were grown on increasing concentrations of methyl methane sulfonate (MMS) or bleomycin (BLM), which both induce DNA strand breaks; MMS creates adducts and apurinic sites, which become single- and double-strand breaks (Schwartz, 1989), while BLM is a radiomimetic drug that creates DSB by a concerted free radical attack on sugar moieties, preferentially attacking adjacent residues on opposite strands (Povirk, 1996).

Serial dilution growth assays show that *hdf*- and *sir*-deficient strains are roughly 100-fold more sensitive to 0.03% MMS than their isogenic parental strain (Figures 3A and 3C). Importantly, the *hdf1sir4* double mutant is also significantly more sensitive than either single mutant (see 0.03% MMS, Figures 3A and 3B). While this implicates both yKu and SIR proteins in survival after damage, their functions appear not to be epistatic. To eliminate possible effects due to *HM* derepression in a haploid background, diploid *sir3* and *sir4* strains were compared to their *SIR*$^+$ parental strain for viability on MMS. Again strains deficient for *sir4*, and to a lesser extent *sir3*, were more sensitive to MMS than the isogenic wild-type strain (Figures 3C and 3D). This was confirmed for two other isogenic pairs of diploid *sir3* and *sir4* strains (data not shown).

When mutant and wild-type strains are cultured on BLM, only *rad52* deficiency confers sensitivity to levels between 10 and 20 mU/ml BLM, and the *hdf*, but not *sir*, strains grow poorly at 30 mU/ml BLM (Figure 3A). Nonetheless, the *hdf1sir4* double mutant is more sensitive than either single mutant, again suggesting that SIR proteins play a role in the repair process distinct from that of yKu. Since the hypersensitivity of *sir* mutants is detected in diploid cells, it cannot simply be due to the coincident expression of *MAT***a**1 and *MAT*α2.

Bleomycin-Induced Damage Delocalizes yKu80p, Rap1p, and Sir4p from Telomeres

We next examined the fate of yKu and SIR proteins under conditions of DNA damage by treating *RAD52*$^+$ strains with a low level of BLM (5 mU/ml). After 3 hr, we observe that the Myc-tagged yKu80p protein has lost its preferential punctate localization in most cells, producing a diffuse nuclear staining (compare −BLM with +BLM, Figure 4A). Similarly, when bleomycin-treated diploid cells are stained for Rap1p, Sir3p, or Sir4p, the

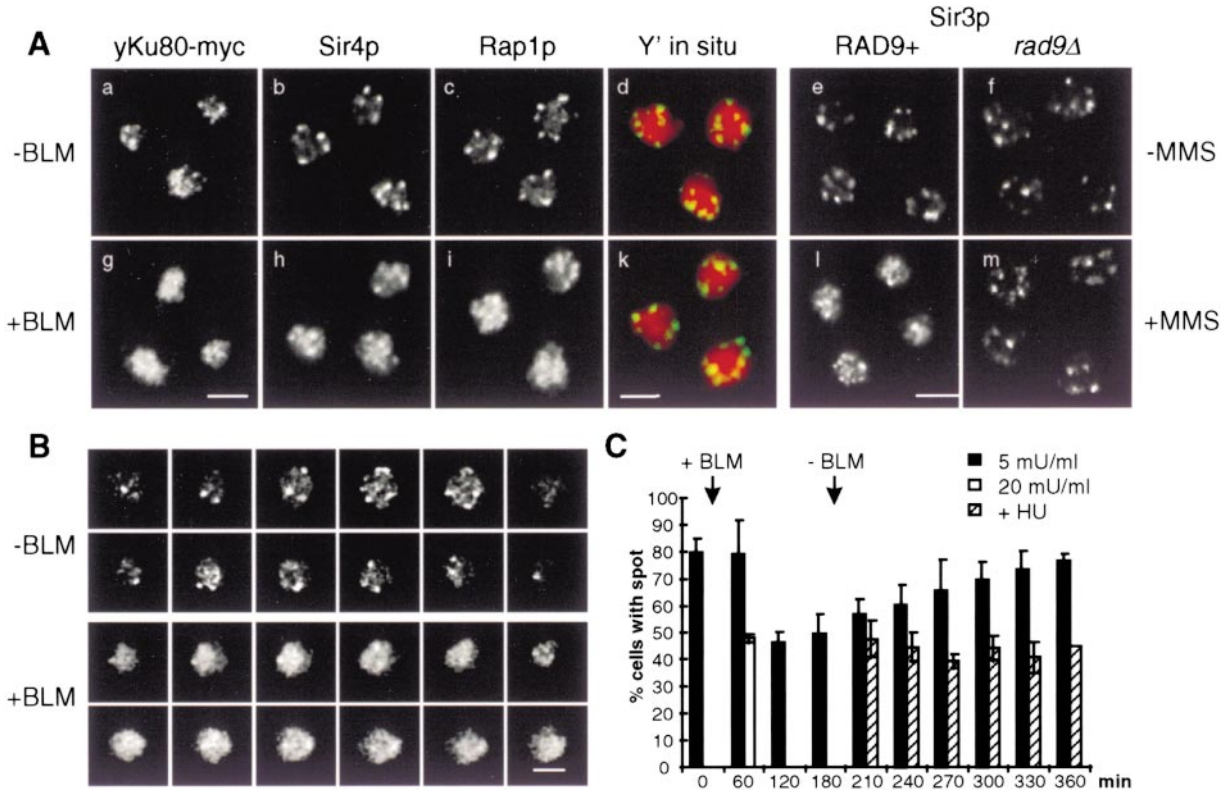

Figure 4. yKu80p, Sir4p, Sir3p, and Rap1p Are Delocalized from Telomeric Foci by Exposure to BLM or MMS in a *RAD9*-Dependent Manner

(A) The haploid Myc-tagged *HDF2* strain (GA 1009, [a and g]) and a diploid wild-type strain (GA 225, [b–d and h–k]) were grown in YPAD (a–d) or in YPAD containing 5 mU/ml of BLM for 3 hr (g–k) and prepared for immunofluorescence or in situ hybridization. The cells were stained with anti-Myc (a and g), affinity-purified anti-Sir4p (b and h), or anti-Rap1p (c and i) antibodies, detected by Texas red–coupled secondary antibody or hybridized with a Y' subtelomeric probe ([d and k]; Y' in situ in green, DNA staining in red). In (e), (f), (l), and (m), a W303 wild-type and isogenic *rad9* deletion strain were grown 3 hr in the presence or absence of 0.03% MMS, prior to fixation and immunostaining with anti-Sir3p (similar results are obtained for Rap1 and Sir4p). Antinuclear pore staining is performed routinely to show that nuclei are still fully intact after drug treatment (data not shown).

(B) A diploid *RAP1-GFP* strain (AHY111) was grown in YPD (−BLM) or incubated 3 hr with 5 mU/ml BLM in YPD (+BLM). Confocal images of living cells are shown. Six sequential focal planes (left to right) are shown for two nuclei of each culture.

(C) AHY111 cells were treated with 5 mU/ml BLM for 0, 60, 120, or 180 min at which points midsection confocal images were taken. Drug was then removed from the culture (see Experimental Procedures) and growth continued in fresh medium for 3 hr. The percentage of cells showing Rap1-GFP spots was scored in each case for 100 cells (black areas) counting only cells that did not have the typical mitotic phenotype, because a subfraction of Rap1p is delocalized in mitosis without damage (T. L., unpublished observations). Some cells were treated with 20 mU/ml BLM (open bar) instead of 5 mU/ml. After removal of BLM, 200 mM HU was added in the fresh medium and cells with wild-type focal patterns of Rap1-GFP were scored as above (hatched bars).

discrete focal staining pattern typical for yeast telomeres is compromised (Figure 4A). To see whether this reflects the disruption of subtelomeric chromatin or a delocalization of telomere sequences, we performed in situ hybridization with a probe for subtelomeric repeats. No alteration in the perinuclear clustering of telomeres is observed in drug-treated cells (Figure 4A), nor is nuclear pore staining altered (data not shown). Finally, Western blot analysis shows that the steady-state levels of Rap1p, SIR proteins, and yKu80 do not increase in the presence of BLM. Confocal sectioning confirms that the three-dimensional structure of the nuclei is preserved despite the diffuse distribution of telomeric proteins (Figure 4B).

The apparent delocalization of telomeric chromatin components in response to DNA damage is observed in both haploid and diploid strains and does not require *rad52* deficiency. A similar dispersed pattern was observed in cells treated with MMS (Figure 4A for Sir3p), although the addition of hydroxyurea, which arrests DNA replication by depleting nucleotide pools, does not alter the focal staining patterns of either Rap1 or the SIR complex (T. L., unpublished observations). Thus, strand breakage, and not the S phase arrest provoked by stalled replication forks, correlates with Rap1p, yKu, and SIR delocalization.

The *RAD9* Checkpoint Triggers Delocalization of Telomere-Associated Proteins

In yeast, DNA damage is sensed by a Rad9p-dependent pathway that signals a cell cycle arrest through the *MEC1*- and *RAD53*-encoded kinases (reviewed by Weinert, 1998). Such checkpoint pathways are critical to ensure chromosomal integrity during mitotic division. Indeed, mutations in the ATM kinase (Mec1p kinase family) are implicated in human diseases that confer a predisposition to cancer (reviewed in Jeggo et al., 1995). To see whether the delocalization of telomeric proteins is

triggered by elements of the checkpoint signaling pathway, we induced DNA damage in a *rad9*-deficient strain and monitored Rap1 and SIR protein localization. In contrast to the isogenic wild-type strain, Rap1p and SIR proteins remain in foci in the *rad9* mutant after treatment with 0.03% MMS (Figure 4A and data not shown); on bleomycin, the *rad9* strain also shows less delocalization (data not shown).

Restoration of Rap1p Foci Requires Passage through S Phase

To test whether the damage-induced telomeric response is reversible and to rule out artefacts such as epitope masking, we have monitored the delocalization of Rap1p in a diploid strain carrying two integrated copies of a *RAP1-GFP* fusion (AHY111). This fusion is fully functional and complements the *rap1* null allele (Hayashi et al., 1998). In these cells we can monitor Rap1 delocalization live by direct GFP epifluorescence.

A series of six 0.3 μm optical sections (from left to right, Figure 4B) shows the nucleus of a living cell, grown in the absence or presence of 5 mU/ml BLM. Consistent with the immunofluorescence results, bright foci of Rap1-GFP are visible primarily at the nuclear periphery in untreated cells, whereas we frequently observe a diffuse Rap1-GFP fluorescence after drug addition. The delocalization phenotype was quantified on an unsynchronized culture, omitting the cells in M phase (dumbbell morphology with dividing nucleus), since we have observed a mitosis-specific delocalization of Rap1p that is independent of DNA damage (T. L. and S. M. G., unpublished data). Less than 50% of the nonmetaphase cells retain discrete Rap1-GFP focal sites in an equatorial section of the cell after 2 hr in the presence of 5 mU/ml BLM (Figure 4C). At higher doses (20 mU/ml) delocalization is more extensive and more rapid. Redistribution of Rap1p is reversible, and normal perinuclear Rap1p foci are restored by 3 hr after removal of the drug (Figure 4C).

Elsewhere we have shown that the delocalization of Rap1p from telomeric foci correlates primarily with its displacement from subtelomeric chromatin, and not from high-affinity binding sites in the TG-rich repeat (Gotta et al., 1996; Strahl-Bolsinger et al., 1997). Thus, we suspected that the delay in the reformation of Rap1p foci after DNA damage might reflect passage through S phase, which was previously shown to be necessary to restore SIR-mediated repression after shifting a *sir3*^{ts} strain to permissive temperature (Miller and Nasmyth, 1984). Indeed, if HU is added after removal of BLM, the number of cells with a dispersed Rap1p pattern remains constant over the subsequent 3 hr (Figure 4C), suggesting again that replication may be necessary to reestablish the focal Rap1p pattern that correlates with TPE. Alternatively, the HU-induced checkpoint may specifically inhibit foci reformation.

A Single Double-Strand DNA Cleavage Elicits a Telomeric Response to DNA Damage

A unique double-strand lesion, such as that provoked by the HO endonuclease, is sufficient to arrest progression of the yeast cell cycle, as part of the *RAD9*-dependent response to DNA damage (Sandell and Zakian, 1993). To see whether a single DSB elicits the redistribution of subtelomeric chromatin components, we made use of a yeast strain bearing an inducible HO endonuclease and a unique recognition site for this enzyme at the *MAT*α locus (gift of S. E. Lee and J. Haber; Figure 5A). Growth on galactose-containing medium induces expression of the HO endonuclease, and cleavage at the *MAT*α locus is essentially complete after 1 hr induction (data not shown, Lee et al., 1998). Deletion of both *HM* loci ensures that this cut can only be repaired by the Ku-dependent end-joining pathway.

Between 2 and 4 hr after induction of the HO endonuclease, the Myc-tagged yKu80p no longer shows a punctate pattern of staining (Figure 5B). Between 4 to 6 hr after the shift to galactose, we see that Rap1p, Sir3p, and Sir4p also assume a similar, diffuse localization (shown for SIRs, Figure 5B). Indeed, double staining for Sir3 and yKu80 at earlier time points reveals a majority of the cells with a diffuse yKu80 staining, surrounded by the typical punctate pattern of telomere-bound Sir3p (yKu80 is green, Sir3p red, Figure 5B). SIR delocalization is not observed in the isogenic strain that lacks the HO endonuclease (see -HO inset), and nuclear pore staining confirms the integrity of nuclear structure (bottom panels, Figure 5B). The fact that a single DSB is sufficient to provoke this reorganization demonstrates that the response is not a mass action or titration effect, consistent with its *RAD9* dependence.

yKu Is Recruited to Sites of Double-Strand Cleavage

To quantitate the delocalization elicited by DNA damage, we performed the ChrIP assay using antibodies recognizing yKu80-Myc or SIR proteins, in the presence and absence of the induced HO endonuclease cleavage. The data are presented as the ratio of a telomere VI R-proximal PCR product (600 bp away from the TG repeats, Figure 6A) to a nontelomeric control fragment (450 bp from within the *SMC2* gene), which serves as an internal standard (neither yKu nor SIR proteins bind *SMC2* specifically). The Tel/SMC ratio is normalized to that detected in the input DNA. In Figure 6A, we show that by 4 hr and 6 hr after induction of HO endonuclease, the enrichment of SIR proteins on the Tel fragment drops by a factor of two. This result confirms that SIR proteins delocalize from subtelomeric chromatin, as seen by immunofluorescence. The ChrIP analysis further indicates that a significant fraction of the SIR complex remains bound to the telomeres even after 6 hr of persistent damage. Similarly, comparative Tel/SMC PCR on yKu80 immunoprecipitates indicates a 2- to 3-fold reduction in telomere-associated yKu80 upon induction of the HO cut (Figure 6A).

We next checked whether yKu or the SIR proteins are recruited to the site of HO cleavage within the *MAT*α locus, using primers that amplify fragments at varying distances from the HO cleavage site (Figure 6B). By 30 min after induction of the endonuclease, we detect a strong enhancement of yKu80 at the HO cut, with the highest enrichment observed for the fragment closest to the cleavage site (HO2/SMC ratio increases 5-fold after 30 min; Figures 6C and 6D). At later time points (4 and 6 hr), quantitation becomes complicated by the fact that the region around the incision becomes recessed

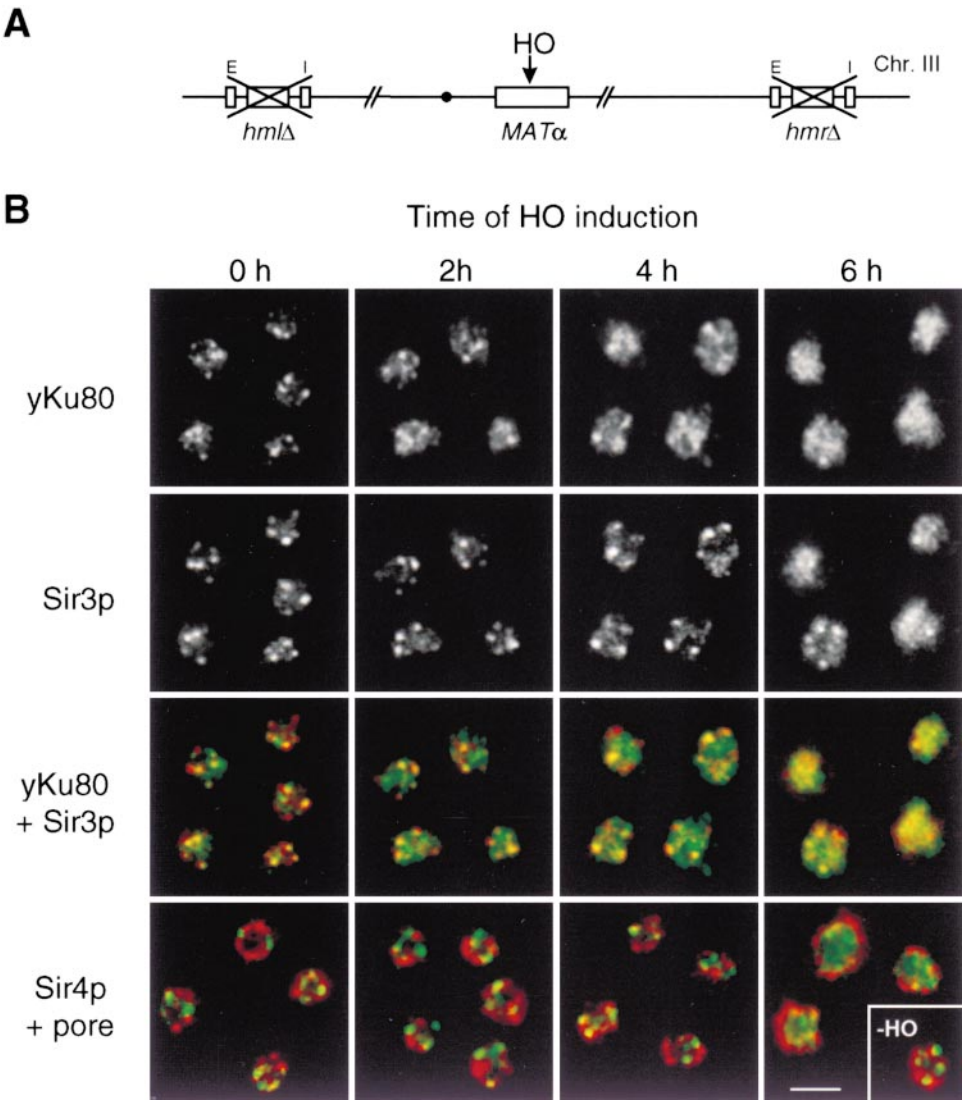

Figure 5. A Single Permanent Double-Strand Cut Elicits Delocalization of Telomere-Associated Proteins

(A) A haploid strain lacking *HM* loci and containing a galactose-inducible HO endonuclease (JKM179) was used such that a single permanent double-strand cut is created on galactose-containing medium. *HDF2* gene was tagged with a 13-mer Myc epitope (GA1139).

(B) Cells were prepared for immunofluorescence after 0, 2, 4, or 6 hr of growth on galactose. GA1139 cells were stained with anti-Myc (9E10) and affinity-purified anti-Sir3p (in the merged image, yKu80-Myc is in green, Sir3p in red), and JKM179 cells were stained with anti-Sir4p (green) and anti-pore (red) antibodies. Western blots indicate no significant increase in yKu80, Rap1, or in Sir3p levels upon HO induction, while Sir4p levels drop slightly (data not shown). The isogenic strain lacking the inducible HO endonuclease (JKM115) was grown on galactose and stained with anti-Sir3p, anti-Sir4p, and anti-Rap1p (inset and data not shown) and shows no delocalizing effects of galactose alone.

by endo- and/or exonucleolytic activity (Lee et al., 1998). This results in a reduced amount of HO signal relative to the SMC standard in the input DNA (see input, Figure 6C; up to 5-fold drop). Accordingly, the intensity of the HO bands drop significantly in relation to the SMC band, in both the yKu and SIR immunoprecipitations as a function of time (Figure 6C). However, normalization of the HO/SMC ratio to that in the input DNA allows us to see that significant levels of yKu are detected near the HO cut at 4 hr, while levels approach background by 6 hr (Figure 6D). Hence, yKu appears to bind a cleavage-site DSB rapidly but transiently. At later time points yKu detection may reflect recruitment to sites that are re-cleaved after a round of repair.

Intriguingly, SIR proteins are not recruited to the HO cleavage site with the same kinetics and efficiency as yKu. There is little or no enrichment of SIR proteins at the *MAT*α locus after 2 hr, whereas yKu levels achieve maximal levels on the cleavage-proximal fragment by 30 min (Figures 6C and 6E). As explained above, in this strain the DSB persists due to the continued expression of HO endonuclease, and the ratio of *MAT*α to the neutral SMC fragment drops during the 6 hr time course. Nonetheless, ratios normalized to the input indicate a 2-fold increase in the presence of Sir3p and Sir4p (when immunoprecipitated individually or together) at *MAT*α flanking sequences after 6 hr of HO induction (Figures 6E and 6F). It is not possible to tell whether the SIR-bound sequences are persistent cuts or sites having undergone repair, although PCR with flanking primers across the

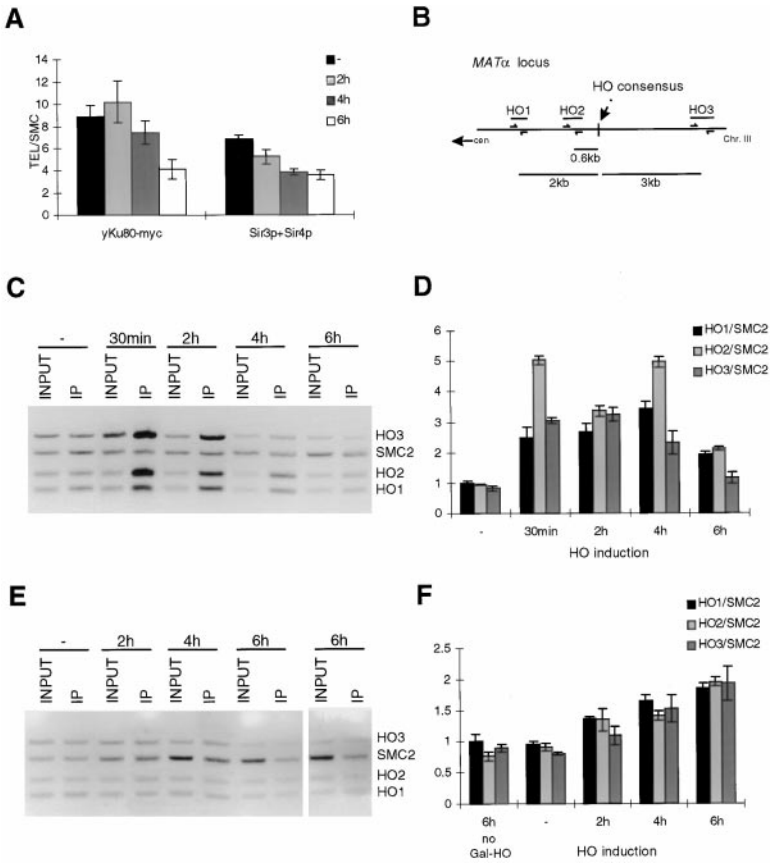

Figure 6. yKu80 and Sir3/4 Proteins Are Recruited with Different Kinetics to a DNA Strand Break

(A) HO endonuclease was induced by growth on galactose for 0, 2, 4, or 6 hr in GA1139 and JKM179. ChrIP assay (see Experimental Procedures) was performed, immunoprecipitating GA1139 DNA with 9E10 (anti-Myc) and JKM179 DNA with affinity-purified anti-Sir3p and anti-Sir4p IgG (mixed). After DNA purification, PCR was performed with primers for a unique sequence near the chromosomal end of VI-R, and for the *SMC2* gene (see Experimental Procedures). The ratio of the telomere signal to the SMC2 signal obtained in the IP samples normalized to this ratio in the INPUT DNA samples is shown. The amount of Sir3/4 bound to telomeres decreases to half the initial value after 6 hr in both strains.

(B) Scheme of the *MAT*α locus showing the pairs of primers used to analyze the recruitment of yKu80 and Sir proteins to the unique HO-cleavage site.

(C) GA1139 strain was prepared as in (A), except that an additional 30 min time point on galactose was prepared and cell extracts were sonicated such that the average DNA fragment size was 2 kb. PCR was performed in parallel on INPUT and yKu80-Myc immunoprecipitated DNA with the mixtures of primers described above. After 4 hr of induction, the HO-proximal signals decrease in the INPUT, due to DSB processing, while the SMC signal remains constant.

(D) Quantitation of the data shown in (C), presented as the ratio of HO-proximal signals to SMC2 in the IP normalized to the same ratio in the corresponding INPUT.

(E) JKM179 cells were prepared as described in (A) and immunoprecipitated with a mixture of antibodies against Sir3p and Sir4p. PCR was identical to that in (C). Although the HO-proximal signals decrease in the INPUT after 4–6 hr due to processing at the DSB, the HO-proximal signals decrease less in the anti-SIR IP, indicating SIR enrichment near the HO-cut site. Two exposures of the 6 hr time point are shown to demonstrate this point.

(F) Quantitation of the data shown in (E), presented as the ratio of HO-proximal signals to *SMC2* in the IP normalized to the same ratio in the corresponding INPUT. Quantitation of a similar experiment using an isogenic strain lacking GAL-HO indicates that galactose alone does not affect SIR localization (first lane).

HO cleavage site indicates that only 6% are intact at 4 or 6 hr after HO induction. A strain lacking GAL-HO shows no increase of SIR binding at *MAT*α after 6 hr on galactose (Figure 6F).

Since roughly half the SIR complexes are released from telomeres after induction of DNA cleavage, the increase in the recovery of HO-bound Sir proteins might simply reflect a higher background of random SIR protein binding, or possibly SIR binding nucleated by an internal Rap1p site. However, the levels of Sir3p or Sir4p associated with the SMC fragment and with a fragment from the *HIS4* promoter that contains a Rap1-binding site are constant even after 6 hr of HO endonuclease expression (data not shown). Thus, the increase in SIR detection at *MAT*α appears to be significant. Strikingly, at early time points where yKu is most highly enriched at the HO cut, we see no significant increase in the binding of SIRs.

DNA Damage Compromises TPE, Displacing Repression-Competent SIR Complexes

As a functional assay for the delocalization of telomeric chromatin components, we monitored the efficiency of subtelomeric repression as compared to internal silencing, under conditions of induced DNA damage. Our reporter strain carries both a telomere-proximal *URA3* reporter and a silencer-flanked *ADE2* gene inserted at the *LYS2* locus, situated 242 kb away from the telomere of Chr. 2 (Figure 7A). Under normal conditions the silencer-flanked internal reporter is expressed, because telomeres sequester SIR proteins at perinuclear foci (Maillet et al., 1996). In the presence and absence of BLM, we score for growth on 5-FOA, which directly monitors the efficiency of telomeric repression (Figure 7B). At 20 or 30 mU/ml BLM, we see a decrease in growth on 5-FOA, indicating a decrease in TPE (Figure 7B). When the drop in viability (see left panel, Figure 7B) is accounted for, TPE is reduced from 42% to 7%, or 6-fold. Derepression could also be detected using a telomere-proximal *ADE2* reporter (data not shown), ruling out *URA3*- or FOA-specific effects. Both assays are consistent with the partial delocalization of SIR complexes observed by ChrIP during HO induction.

To determine whether the displaced SIR proteins are still competent for repression, we monitored repression of the internal silencer-flanked *ADE2* reporter in the

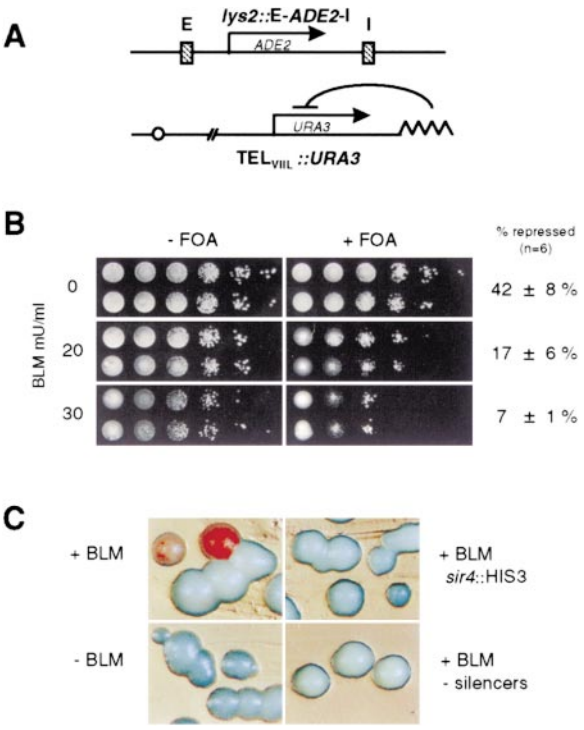

Figure 7. DNA Damage Impairs TPE While Improving Internal Silencer-Mediated Repression

(A) To monitor TPE and internal silencing, the haploid LM11 strain containing a telomere-proximal *URA3* gene (TEL_{VIIL}::*URA3*), and an *HML* E and I silencer-flanked *ADE2* gene inserted at the *LYS2* locus (*lys2*::E-*ADE2*-I) were used.

(B) Serial dilutions of LM11 were plated on complete medium with or without 5-FOA with increasing concentrations of BLM, as indicated. The inhibition of growth on BLM is taken into consideration in the calculation of the percentage of colonies that repress *URA3* (FOA resistance, indicated at right). The mean and standard deviation are calculated from six independent experiments.

(C) Colonies growing on 20 mU/ml BLM accumulate red pigment, as they repress the silencer-flanked internal *ADE2* reporter gene (+BLM; top left). No red colonies were scored in LM11 with a *sir4* disruption (+BLM, *sir4*Δ; top right; GA1056), when *ADE2* lacks adjacent silencers (+BLM; bottom right; GA187), or in absence of BLM (bottom left).

presence of bleomycin. Indeed, we observe an accumulation of red pigment in these colonies, which is not present in the absence of damage (Figure 7C, upper left corner). This repression requires the intact SIR complex, the presence of the flanking silencer elements, and correlates with the bleomycin-induced release of SIR proteins from telomeric foci (Figure 7C). Thus, we conclude that a significant fraction of the displaced SIR proteins are competent to form repressed chromatin and can be recruited by silencers to internal chromosomal sites.

In summary, our data suggest that DNA damage elicits a change in telomeric heterochromatin, although internal silencer-mediated repression remains intact. A checkpoint-induced change in SIR-yKu interaction would provide a mechanism to release yKu and SIR proteins from subtelomeric sequences. The modified yKu would then be free to scan the damaged genome for DSB and may under these conditions preferentially interact with Mre11 and the Ligase IV complex.

Discussion

Double-strand breaks are highly deleterious to the integrity of the genome, and improper processing or repair of DSB can lead to gene rearrangements, deletions, or aneuploidy. Indeed, the eukaryotic cell has developed elaborate means to eliminate DSB without loss of information, through homologous recombination and/or direct end-joining reactions. Both pathways require an arrest in cell cycle progression until the chromosome is repaired, which is imposed by the DNA damage checkpoint (Weinert, 1998).

Telomeric Domains Respond to the DNA Damage Checkpoint Signal

In this paper, we document a surprising redistribution of yeast telomeric and subtelomeric chromatin components in response to DNA damage. Three independent assays, namely immunofluorescence, chromatin immunoprecipitation, and transcriptional repression, confirm that a significant fraction of the histone-binding SIR complex is displaced from subtelomeric sequences, where it is normally sequestered in perinuclear foci. The delocalization of SIR proteins occurs in response to MMS, bleomycin, and following the induction of a single double-strand cut mediated by the HO endonuclease. Irradiation by UV (Mills et al., 1999 [this issue of *Cell*]) and treatment with hydroxyurea do not have equivalent effects, suggesting that the response is specific for DNA strand breaks. Importantly, the relocalization of SIR proteins is abrogated by deletion of *RAD9*, implicating the DNA damage checkpoint in the response.

In addition to the SIR complex, subpopulations of the DNA-binding Rap1p and yKu proteins are released upon induction of a single DSB. The delocalization of Rap1p could have been expected, since immunofluorescence and chromatin cross-linking assays identified a subpopulation of Rap1p that binds telomeres in a SIR-dependent manner (Palladino et al., 1993; Gotta et al., 1996; Strahl-Bolsinger et al., 1997). We show here that yKu propagates inward along Chr. VI-R to roughly the same extent as SIR and Rap1p, suggesting that the release of yKu may reflect its loss from subtelomeric regions and not from the more distal TG repeats (Figure 1). These observations provide support for the model that subtelomeric heterochromatin serves as a reservoir for proteins that are released to act at other nuclear sites in response to physiological signals. In the case of DSB, one might argue that a checkpoint-induced release of yKu ensures sufficient protein for a rapid scanning of the genome to minimize inappropriate recombination or fusion events.

The subtelomeric reservoir model is based on the finding that internal, silencer-flanked reporters (including reporters at the *HM* loci) compete with TPE for the limiting pool of Sir3p and Sir4p (Maillet et al., 1996; Marcand et al., 1996). rDNA repeats also compete with telomeres for limiting amounts of Sir2p (Cockell et al., 1998). However, until this study, the only evidence indicating that SIR relocalization might be physiologically relevant was the observation that Sir3p and Sir4p migrate to the nucleolus in aging yeast cells and in mutants that extend their average maximal number of divisions (Kennedy et al., 1997). In the case of aging, the accumulation of excised rDNA circles may recruit Sir3p and

Sir4p from telomeres, provoking a concomitant loss of TPE. From the data shown here, we propose that signaling through the DNA damage checkpoint elicits the release of yKu and SIR proteins from complexes associated with subtelomeric heterochromatin.

Potential Roles for SIR Protein Release in DSB Repair

Why release a subfraction of SIR complexes in response to DNA damage? It is possible that SIR protein delocalization is a meaningless side effect of the release of yKu, which is known to play a direct role in DSB repair. Two results argue against this. First, Mills et al. (1999) and Tsukamoto et al. (1997) have demonstrated that *sir*-deficient strains are significantly less efficient in an NHEJ assay than isogenic *SIR*$^+$ strains. Second, we show that *sir*-deficient haploid and diploid strains are reproducibly hypersensitive to MMS. BLM sensitivity is less pronounced for *sir* mutants than for strains lacking yKu, and yet the impairment to growth is additive in the double mutant, suggesting that *HDF1* and *SIR4* are both involved, but are not epistatic, in some aspect of DSB repair.

SIR Proteins Are Recruited to an HO Cleavage Site with Different Kinetics Than yKu

Earlier studies have proposed that yKu targets the SIR complex to sites of damage to protect flanking DNA from the transcriptional apparatus (Jackson, 1997). However, in view of the kinetics of protein release from telomeres and of yKu and SIR protein association at the HO cut, we suggest a somewhat different scenario. The maximal level of yKu recruitment (30 min after HO induction) persists until 4 hr, yet by 6 hr yKu is no longer significantly enriched at *MAT*α. In the case of SIR proteins, association near the cleavage site at 2 hr is negligible ($<$1.2-fold), but increases continually, reaching $\sim$2-fold at 6 hr after HO induction. These dissimilar kinetics do not support the idea that yKu directly targets SIR complexes to sites of DSB. Consistently, we have seen that although GBD-yKu is extremely efficient at nucleating SIR-mediated silencing at internal sites under normal growth conditions (Figure 2), yKu-mediated repression is compromised on MMS (data not shown). This is not due to inactivation of the SIR complex, since GBD-Sir2p functions efficiently to nucleate SIR-mediated repression in the presence of DNA-damaging agents. One interpretation of this is that the interaction between yKu and the SIR complex is modified during the cellular response to DNA damage, possibly by phosphorylation. The close association of Ku with DNA-PK in mammalian cells makes it likely that yKu is recognized by an ATM homolog in yeast (Mec1 or Tel1). Such a modification may interfere with yKu recruitment of the SIR complex to sites of DNA damage.

As an alternative hypothesis, we propose that the release of SIR complexes from subtelomeric regions and its recruitment to sites of repair reflect association with newly assembled chromatin. It has been demonstrated that the nucleosome assembly factor CAF1 is recruited to sites of DNA damage in mammalian cells (Martini et al., 1998), and its role in nucleosome assembly following DNA repair is well documented (Gaillard et al., 1996). Mutation of the yeast equivalent of the mammalian CAF1 (*CAC1*) intriguingly shows a derepression of TPE and hypersensitivity to DNA damage (Enomoto et al., 1997; Kaufman et al., 1997). Since DSB repair involves extensive resynthesis of DNA and hence nucleosome assembly, we propose that the recruitment of SIR complexes reflects the assembly of a repressed chromatin state following DNA repair. It is not known whether CAF1 or another complex assembles nucleosomes after NHEJ reactions, yet this pathway would be consistent with the kinetics of SIR association at cleavage sites and the well-characterized interaction of SIR proteins with nucleosomes. Such a mechanism might prevent the spurious activation of genes as a result of DNA repair. It will be interesting to test whether SIR proteins are still targeted to the HO cut in a *cac1* deletion strain.

Adapting to a DSB

In view of the physical similarity of DSB and telomeric termini, such damage presents a unique challenge to the cell's repair pathway. It has been demonstrated that cells with irreparable damage downregulate Rad9p after 6–8 hr and proceed through the cell cycle in a process called adaptation (Sandell and Zakian, 1993; Toczyski et al., 1997; Lee et al., 1998). Since the timing of the SIR protein recruitment to an irreparable HO cleavage site correlates with this event, it is possible that the binding of SIRs may help protect the unrepaired end from further degradation, as the cells proceed through mitosis (Sandell and Zakian, 1993). Thus, the unexpected checkpoint-elicited release of telomere-associated chromatin factors may reflect their involvement in adaptation to persistent DNA damage, a phenomenon implicated in mammalian oncogenesis.

Experimental Procedures

Media

Yeast strains were grown using standard conditions (Rose et al., 1990). Bleomycin (Sigma Chemicals, Buchs, Switzerland) was diluted to 10 U/ml in H_2O. For plates containing BLM, 5-FOA, or MMS, drugs were added to cooled media. For immunofluorescence studies, 5 mU/ml BLM, 0.03% MMS, or 200 mM hydroxyurea was added for 3 hr prior to fixation unless otherwise stated. For HO endonuclease induction, strains were grown on rich medium containing 3% glycerol, 2% lactic acid, and 0.05% glucose, prior to adding 2% galactose.

Strains

Genotypes of yeast strains are described in Table 1. To create GA1009 and GA1139, a 13-mer Myc epitope was amplified from pFA6a-13Myc-kanMX6 (Longtine et al., 1998) and recombined into the C terminus of *HDF2* in GA426 (formerly UCC3107, Aparicio et al., 1991), and JKM179 (Lee et al., 1998), respectively. Correct insertion was confirmed by Western blot and analytical PCR. GA1050 was created by transformation of GA426 with a *rad52::URA3* construct, and GA1065 was created by disruption of GA911 with pJR276 (*sir4::HIS3*). The LM11 strain (a gift of L. Maillet and E. Gilson, ENS, Lyon, France) carries both a VIIL telomere-proximal *URA3* reporter and a wild-type *ADE2* gene flanked on either side by 1.5 kb of sequence containing the *HML* E and I silencers, integrated at *LYS2*, to allow the monitoring of silencer-mediated repression at an internal chromosomal site (Maillet et al., 1996). GA1056 and GA1061 were obtained by disrupting *SIR4* in LM11 and GA1009, respectively, using pJR276 (*sir4::HIS3*; Kimmerly and Rine, 1987). Correct insertion was checked by Southern blot.

Ce134 (E-I), Ce76 (E-Δi), and Ce77 (Δe-Δi) strains are gifts from G. Fourel and E. Gilson (ENS, Lyon). Four double Gal4p recognition sites were inserted upstream of the *URA3* gene, which is placed

Table 1. Yeast Strains Used in This Study

Name	Genotype	Reference
GA192	*MAT***a**/*MAT*α *ade2-1/ADE2 his3/his3 leu2-3/LEU2 lys2-6/LYS2 trp1/TRP1 ura3-1/ura3-52 can1/CAN1 sir3::TRP1/sir3::LYS2*	Gotta et al., 1996
GA202	*MAT***a**/*MAT*α *ade2-1/ADE2 his3/his3 leu2-3/LEU2 lys2-6/LYS2 trp1/trp1 ura3-1/ura3-52 can1/CAN1 sir4::HIS3/sir4::HIS3*	Gotta et al., 1996
GA225	*MAT***a**/*MAT*α *ade2-1/ADE2 his3/his3 leu2-3/LEU2 trp1/TRP1 ura3-1/ura3-52 can1/CAN1*	Gotta et al., 1996
GA426	*MAT***a** *ade2::hisG his3-11 leu2 trp1 ura3-52 can1::hisG VR::ADE2-TEL*	H. Renauld, unpublished data
GA427	GA426 *sir2::HIS3*	H. Renauld, unpublished data
GA428	GA426 *sir3::HIS3*	H. Renauld, unpublished data
GA429	GA426 *sir4::HIS3*	H. Renauld, unpublished data
GA911	GA426 *hdf1::kanMX*	Laroche et al., 1998
GA1065	GA426 *hdf1::kanMX sir4::HIS3*	This study
GA1050	GA426 *rad52::URA3*	This study
GA1009	GA426 *HDF2-myc(::kanMX4)*	This study
GA1061	GA426 *HDF2-myc(::kanMX4) sir4::HIS3*	This study
W303a	*MAT***a** *ade2-1 leu2-3,112 his3-11,15 trp1 ura3-1 can1-100*	
YT29	*W303a hdf1::kanMX4*	Laroche et al., 1998
S114	*W303a rad9::LEU2*	D. Shore, unpublished data
AHY111	*MAT***a**/*MAT*α *arg4/arg4 leu2::hisG/leu2::hisG ura3/ura3 ho::LYS2/ho::LYS2 RAP1-GFP-LEU2::rap1/RAP1-GFP-LEU2::rap1*	Hayashi et al., 1998
JKM115	*MAT*α *ade1 leu2-3,112 lys5 trp1::hisG ura3-52 hml::ADE1 hmr::ADE1*	Lee et al., 1998
JKM179	JKM115 *ade3::GALHO*	Lee et al., 1998
GA1139	JKM115 *ade3::GALHO HDF2-myc(::kanMX4)*	This study
LM11	*MAT*α *ade2-1 his3-11,115 leu2-3,112 trp1-1 ura3-1 can1-100 TelVII::URA3 lys2::HMLEI::ADE2*	L. Maillet and E. Gilson, unpublished data
GA1056	LM11 *sir4::HIS3*	This study
Ce134	*MAT***a** *his3*Δ *leu2-3,112 trp1 ura3-52 gal2 hml::E-GalUAS2-URA3-I*	G. Fourel and E. Gilson, unpublished data
Ce76	*MAT***a** *his3*Δ *leu2-3,112 trp1 ura3-52 gal2 hml::E-GalUAS2-URA3-*Δi	G. Fourel and E. Gilson, unpublished data
Ce77	*MAT***a** *his3*Δ *leu2-3,112 trp1 ura3-52 gal2 hml::*Δ*e-GalUAS2-URA3-*Δ*i*	G. Fourel and E. Gilson, unpublished data

between the *HML* E and I silencers, and deletions in Ce76 and Ce77 remove the full silencers (Boscheron et al., 1996).

Plasmids

The pGBT9-ORC1 plasmid encodes the first 238 aa of Orc1p fused in-frame to the Gal4p-binding domain (GBD, gift of C. Boscheron and E. Gilson, ENS, Lyon). The pGBT9-SIR2 plasmid contains the entire *SIR2* gene fused in-frame to GBD (gift of M. Cockell, ISREC). pGBD-yKu fusions were created by cloning *HDF1* and *HDF2* genes amplified by PCR into pAS2 (2 μm-*TRP1*; Clontech). pGBD-HDF1 fully complements an *hdf1* deletion for TPE and viability at 37°C, whereas pGBD-HDF2 complements a *hdf2* null for temperature sensitivity.

Immunofluorescence and In Situ Hybridization

Published methods and antibodies were used for immunofluorescence, $Y'+TG_{1\text{–}3}$ repeat in situ hybridization, and confocal imaging (Gotta et al., 1996). All rabbit sera were affinity purified prior to use. Other antibodies were as follows: anti-Myc (9E10), anti-p62 monoclonal antibody (Mab414; Berkeley Antibody Corp.), DTAF- or Texas red–conjugated secondary antibody (Jackson ImmunoResearch Laboratories), Cy5-coupled reagents (Milan Analytica), and fluorescein-derivatized sheep anti-digoxigenin (DIG) F(ab) fragments (Roche Diagnostics). Secondary antibodies are preadsorbed against fixed yeast spheroplasts prior to use.

ChrIP

The extraction and sonication of formaldehyde-fixed yeast cells were done essentially as described in Strahl-Bolsinger et al. (1997). For telomere analyses (Figure 1), the average size of sonicated DNA was ~500 bp, and PCR primers were identical to those described (Strahl-Bolsinger et al., 1997). For analyses of the HO cleavage site, the average size fragment was ~2 kb due to less extensive sonication. Immunoprecipitation was performed with precoated Dynabeads overnight at 4°C. An aliquot of each sample was not immunoprecipitated (Input). Input and immunoprecipitated samples were incubated for 6 hr at 65°C to revert the formaldehyde cross-linking, prior to DNA purification and semiquantitative PCR. Primers used are specific for the 3 kb region downstream of the HO cleavage site in MATα (SG420: 5′-AAGTGCTCCCAATAGGCG GTTTCTC-3′ and SG421: 5′-TTGATGCCGAGGACG AAGTAGAGGA-3′), producing a 560 bp fragment (HO3), and for regions 0.6 kb and 2 kb upstream from the HO cleavage site (SG422 5′-AGTATGCTGGATTTAAACTCA TCTGTGATTTGTGG-3′ and SG122 5′-GCAGGCTTCGAAGTAAA CATATTGTGAATGTCG-3′, producing a 350 bp fragment, HO2; SG418 5′-CTTGTATTAGACGAGGGACGGAGTG-3′ and SG419 5′-ACAGAGGGTCACAGCACTACTACAG-3′, producing a 290 bp fragment, HO1). The Chr VI-R telomere primers (SG355: 5′-CACCGC CAAGCTTCCAATATCACG-3′ and SG356: 5′-GGAGGCATTATGGC TTTGTTACGC-3′) produce a 400 bp fragment located 0.6 kb from the TG repeat, and primers from *SMC2* (SG139: 5′-AAGAGAAACTTT AGTCAAAACATGGG-3′ and SG135: 5′-CCATCACATTATACTAACT ACGG-3′) produce the 450 bp internal standard. PCR products were resolved by electrophoresis and assayed by densitometry using AIDA (Fuji) or Phosphorimager, as indicated.

Silencing and Viability Assays

The expression of the telomere-proximal *URA3* or the *GAL-URA3* construct at *HML* was monitored by determining the fraction of cells capable of growth after 3–5 days at 30°C on 0.1% 5-FOA-containing medium, which allows growth of cells that fail to express *URA3* (Gottschling et al., 1990). Mean and standard deviation were calculated from multiple titrations of at least four independent colonies. For the *ADE2* reporter, cells were grown on medium with limiting adenine.

Acknowledgments

We acknowledge invaluable help from M. Tsai-Pflugfelder (ISREC) for the ChrIP assay. We are grateful to E. Gilson, L. Maillet, G. Fourel, C. Boscheron (all ENS, Lyon, France), and H. Renauld and M. Cockell (ISREC) for unpublished plasmids and strains. We thank J. Haber and D. Shore for published yeast strains, J. Lingner and members of the Gasser laboratory for helpful discussions, and K. Mills and L. Guarente for sharing information prior to submission. The Gasser laboratory thanks the Swiss National Science Foundation, Human

Frontier Science Program, and the Swiss Cancer League for support, and the Grunstein laboratory acknowledges the Human Frontier Science Program and a grant from National Institutes of Health.

Received March 8, 1999; revised April 23, 1999.

References

Andrulis, A.D., Neiman, A.M., Zappulla, D.C., and Sternglanz, R. (1998). Perinuclear localization of chromatin facilitates transcriptional silencing. Nature *394*, 592–595.

Aparicio, O.M., Billington, B.L., and Gottschling, D.E. (1991). Modifiers of position effect are shared between telomeric and silent mating-type loci in S. cerevisiae. Cell *66*, 1279–1287.

Aström, S.U., Okamura, S.M., and Rine, J. (1999). Yeast cell-type regulation of DNA repair. Nature *397*, 310.

Boscheron, C., Maillet, L., Marcand, S., Tsai-Pflugfelder, M., Gasser, S.M., and Gilson, E. (1996). Cooperation at a distance between silencers and proto-silencers at the yeast HML locus. EMBO J. *15*, 2184–2195.

Boulton, S.J., and Jackson, S.P. (1998). Components of the Ku-dependent non-homologous end-joining pathway are involved in telomeric length maintenance and telomeric silencing. EMBO J. *17*, 1819–1828.

Cockell, M., Gotta, M., Palladino, F., Martin, S.G., and Gasser, S.M. (1998). Targeting Sir proteins to nuclear domains: a general mechanism for transcriptional repression. Cold Spring Harb. Symp. Quant. Biol. *63*, 401–412.

Critchlow, S.E., and Jackson, S.P. (1998). DNA end-joining: from yeast to man. Trends Biochem. Sci. *23*, 394–398.

Dynan, W.S., and Yoo, S. (1998). Interaction of Ku protein and DNA-dependent protein kinase catalytic subunit with nucleic acids. Nucleic Acids Res. *26*, 1551–1559.

Enomoto, S., McCune-Zierath, P.D., Gerami-Nejad, M., Sanders, M.A., and Berman, J. (1997). *RLF2*, a subunit of yeast chromatin assembly factor-I, is required for telomeric chromatin function *in vivo*. Genes Dev. *11*, 358–370.

Gaillard, P.H., Martini, E.M., Kaufman, P.D., Stillman, B., Moustacchi, E., and Almouzni, G. (1996). Chromatin assembly coupled to DNA repair: a new role for chromatin assembly factor I. Cell *86*, 887–896.

Gotta, M., Laroche, T., Formenton, A., Maillet, L., Scherthan, H., and Gasser, S.M. (1996). The clustering of telomeres and colocalization with Rap1, Sir3 and Sir4 proteins in wild-type Saccharomyces cerevisiae. J. Cell Biol. *134*, 1349–1363.

Gottschling, D.E., Aparicio, O.M., Billington, B.L., and Zakian, V.A. (1990). Position effect at S. cerevisiae telomeres: reversible repression of Pol II transcription. Cell *63*, 751–762.

Gravel, S., Larrivee, M., Labrecque, P., and Wellinger, R.J. (1998). Yeast Ku as a regulator of chromosomal DNA end structure. Science *280*, 741–744.

Gu, Y., Seidl, K.J., Rathbun, G.A., Zhu, C., Manis, J.P., van der Stoep, N., Davidson, L., Cheng, H.L., Sekiguchi, J.M., Frank, K., et al. (1997). Growth retardation and leaky SCID phenotype of Ku70-deficient mice. Immunity *7*, 653–665.

Haber, J.E. (1998). The many interfaces of Mre11. Cell *95*, 583–586.

Hayashi, A., Ogawa, H., Kohno, K., Gasser, S.M., and Hiraoka, Y. (1998). Meiotic behaviours of chromosomes and microtubules in budding yeast: relocalization of centromeres and telomeres during meiotic prophase. Genes Cells *3*, 587–601.

Jackson, S.P. (1997). Genomic stability: silencing and DNA repair connect. Nature *388*, 829–830.

Jeggo, P.A., Taccioli, G.E., and Jackson, S.P. (1995). Menage a trois: double strand break repair, V(D)J recombination and DNA-PK. Bioessays *17*, 949–957.

Kaufman, P.D., Kobayashi, R., and Stillman, B. (1997). Ultraviolet radiation sensitivity and reduction of telomeric silencing in Saccharomyces cerevisiae cells lacking chromatin assembly factor-I. Genes Dev. *11*, 345–357.

Kennedy, B.K., Gotta, M., Sinclair, D.A., Mills, K., McNabb, D.S., Murthy, M., Pak, S.M., Laroche, T., Gasser, S.M., and Guarente, L. (1997). Redistribution of silencing proteins from telomeres to the nucleolus is associated with extension in life span in *S. cerevisiae*. Cell *89*, 381–391.

Kimmerly, W.J., and Rine, J. (1987). Replication and segregation of plasmids containing cis-acting regulatory sites of silent mating-type genes in Saccharomyces cerevisiae are controlled by the SIR genes. Mol. Cell. Biol. *7*, 4225–4237.

Laroche, T., Martin, S.G., Gotta, M., Gorham, H.C., Pryde, F.E., Louis, E.J., and Gasser, S.M. (1998). Mutation of yeast Ku genes disrupts the subnuclear organization of telomeres. Curr. Biol. *8*, 653–656.

Lee, S.E., Moore, J.K., Holmes, A., Umezu, K., Kolodner, R.D., and Haber, J.E. (1998). *Saccharomyces* Ku70, mre11/rad50 and RPA proteins regulate adaptation to G2/M arrest after DNA damage. Cell *94*, 399–409.

Lieber, M.R., Grawunder, U., Wu, X., and Yaneva, M. (1997). Tying loose ends: roles of Ku and DNA-dependent protein kinase in the repair of double-strand breaks. Curr. Opin. Genet. Dev. *7*, 99–104.

Longtine, M.S., McKenzie, A., III, Demarini, D.J., Shah, N.G., Wach, A., Brachat, A., Philippsen, P., and Pringle, J.R. (1998). Additional modules for versatile and economical PCR-based gene deletion and modification in Saccharomyces cerevisiae. Yeast *14*, 953–961.

Mages, G.J., Feldmann, H.M., and Winnacker, E.L. (1996). Involvement of the *Saccharomyces cerevisiae* HDF1 gene in DNA double-strand break repair and recombination. J. Biol. Chem. *271*, 7910–7915.

Maillet, L., Boscheron, C., Gotta, M., Marcand, S., Gilson, E., and Gasser, S.M. (1996). Evidence for silencing compartments within the yeast nucleus: a role for telomere proximity and Sir protein concentration in silencer-mediated repression. Genes Dev. *10*, 1796–1811.

Marcand, S., Buck, S.W., Moretti, P., Gilson, E., and Shore, D. (1996). Silencing of genes at nontelomeric sites in yeast is controlled by sequestration of silencing factors at telomeres by Rap 1 protein. Genes Dev. *10*, 1297–1309.

Martini, E., Roche, D.M., Marheineke, K., Verreault, A., and Almouzni, G. (1998). Recruitment of phosphorylated chromatin assembly factor 1 to chromatin after UV irradiation of human cells. J. Cell Biol. *143*, 563–575.

Miller, A.M., and Nasmyth, K.A. (1984). Role of DNA replication in the repression of silent mating type loci in yeast. Nature *312*, 247–251.

Mills, K.D., Sinclair, D.A., and Guarente, L. (1999). *MEC1*-dependent redistribution of the Sir3 silencing protein from telomeres to DNA double-strand breaks. Cell *97*, this issue, 609–620.

Nugent, C.I., Bosco, G., Ross, L.O., Evans, S.K., Salinger, A.P., Moore, J.K., Haber, J.E., and Lundblad, V. (1998). Telomere maintenance is dependent on activities required for end repair of double-strand breaks. Curr. Biol. *8*, 657–660.

Nussenzweig, A., Chen, C., da Costa Soares, V., Sanchez, M., Sokol, K., Nussenzweig, M.C., and Li, G.C. (1996). Requirement for Ku80 in growth and immunoglobulin V(D)J recombination. Nature *382*, 551–555.

Palladino, F., Laroche, T., Gilson, E., Axelrod, A., Pillus, L., and Gasser, S.M. (1993). SIR3 and SIR4 proteins are required for the positioning and integrity of yeast telomeres. Cell *75*, 543–555.

Polotnianka, R.M., Li, J., and Lustig, A.J. (1998). The yeast Ku heterodimer is essential for protection of the telomere against nucleolytic and recombinational activities. Curr. Biol. *8*, 831–834.

Porter, S.E., Greenwell, P.W., Ritchie, K.B., and Petes, T.D. (1996). The DNA-binding protein Hdf1p (a putative Ku homologue) is required for maintaining normal telomere length in Saccharomyces cerevisiae. Nucleic Acids Res. *24*, 582–585.

Povirk, L.F. (1996). DNA damage and mutagenesis by radiomimetic DNA-cleaving agents: bleomycin, neocarzinostatin and other enediynes. Mutat. Res. *355*, 71–89.

Rose, M.D., Winston, F., and Hieter, P. (1990). Methods in Yeast Genetics (Cold Spring Harbor, NY: Cold Spring Harbor Laboratory Press).

Sandell, L.L., and Zakian, V.A. (1993). Loss of a yeast telomere: arrest, recovery, and chromosome loss. Cell *75*, 729–739.

Schwartz, J.L. (1989). Monofunctional alkylating agent-induced S-phase-dependent DNA damage. Mutat. Res. *216*, 111–118.

Shore, D. (1998). Telomeres—unsticky ends. Science *281*, 1818–1819.

Siede, W., Friedl, A.A., Dianova, I., Eckardt-Schupp, F., and Friedberg, E.C. (1996). The *Saccharomyces cerevisiae* Ku autoantigen homologue affects radiosensitivity only in the absence of homologous recombination. Genetics *142*, 91–102.

Strahl-Bolsinger, S., Hecht, A., Kunheng, L., and Grunstein, M. (1997). SIR2 and SIR4 interactions differ in core and extended telomeric heterochromatin in yeast. Genes Dev. *11*, 83–93.

Toczyski, D.P., Galgoczy, D.J., and Hartwell, L.H. (1997). CDC5 and CKII control adaptation to the yeast DNA damage checkpoint. Cell *90*, 1097–1106.

Tsukamoto, Y., Kato, J., and Ikeda, H. (1997). Silencing factors participate in DNA repair and recombination in S. cerevisiae. Nature *388*, 900–903.

Weinert, T. (1998). DNA damage checkpoints update: getting molecular. Curr. Opin. Genet. Dev. *8*, 185–193.